Proceedings of the Twenty-eighth (2018) International Ocean and Polar Engineering Conference
Sapporo, Japan, June 10-15, 2018

ISBN 978-1-880653-87-6; ISSN 1098-6189

www.isope.org

Mating Control of a Wind Turbine Tower-Nacelle-Rotor Assembly for a Catamaran Installation Vessel

Zhiyu Jiang[1,2], *Zhengru Ren*[1,2,3], *Zhen Gao*[1,2,3]
Peter Christian Sandvik[2,4], *Karl Henning Halse* [2,5], *Roger Skjetne*[1,2,3]
1 Department of Marine Technology, Norwegian University of Science and Technology (NTNU), Trondheim, Norway
2 Centre for Research-based Innovation of Marine Operations (SFI MOVE), NTNU
3 Centre for Autonomous Marine Operations and Systems (SFF AMOS), NTNU, Trondheim, Norway
4 PC Sandvik Marine, Trondheim, Norway
5 Department of Ocean Operations and Civil Engineering, NTNU, Ålesund, Norway

ABSTRACT

The assembly and installation costs of an offshore wind farm can approach 20% of the capital expenditures; therefore, time efficient installation methods are needed for installing offshore wind turbines. This study investigates the feasibility of a novel wind turbine installation concept using a catamaran. The catamaran is designed to carry wind turbine assemblies on board and to perform installation using lifting grippers. The installation of a rotor-tower-assembly onto a spar foundation is considered with a focus on the mating process of a tower-nacelle-rotor assembly. The spar foundation has been pre-installed at a representative site in the North Sea, and the catamaran has thrusters regulated by a dynamic positioning system. Numerical modelling of various components of the concept are introduced. Time-domain simulations of the system are performed in irregular waves, and the relative motion and velocity between the tower bottom and the spar top are analysed during the mating process. It was found that the active heave compensator can effectively reduce the relative heave velocity and the risks of structural damage during the mating process.

KEY WORDS: Offshore wind turbine installation; catamaran; mating; active heave compensator; motion control.

INTRODUCTION

The offshore wind industry has witnessed continuous growth in the past decade. To improve the cost effectiveness of offshore wind power, there is a trend to design larger wind turbines for greater water depths. Various types of supporting structures have been proposed for offshore wind turbines (OWTs). Generally, for water depth less than 40 meters, monopile, gravity-based, and jacket foundations are the most commercially competitive (Pieda and Tardieu, 2010). For water depths greater than 100 m, floating foundations including spar, semisubmersible, and tension leg platforms are viable solutions, although their commercialisation is still at a preliminary stage because of costs.

Offshore installation is expensive. According to a recent study (Moné et al., 2017), the assembly and installation cost contributes approximately 20% to the capital expenditures of a bottom-fixed offshore wind farm. The installation costs are partly due to the rental of installation vessels and weather-restrictive nature of traditional marine operations (e.g. significant wave height $\leq$ 2.0 m). The turbulent wind condition is another factor that poses constraints. To avoid delays during offshore installation and to increase profit margins of the offshore wind industry, innovative and cost-effective methods for installing OWTs are desired. For instance, Sarkar and Gudmestad (2017) suggested an installation approach using a floating vessel with a floatable subsea structure for installation of monopile-type wind turbines. Guachamin-Acero et al. (2017) proposed another method for installing bottom-fixed wind turbines based on the inverted pendulum principle. Yet, these installation methods are not readily applicable to floating wind turbines.

A novel concept was proposed in the SFI MOVE project for installing bottom-fixed and floating OWTs (Hatledal et al., 2017). This concept utilises a catamaran vessel which carries a maximum of four tower-nacelle-rotor assemblies in an installation task. Unlike the split method (Jiang et al., 2018a) which requires several lifts of blades or nacelle, the catamaran installation concept is more efficient - it requires only one lift for each wind turbine assembly. Figure 1 illustrates a visual impression of this concept during an installation task. In general, the procedure for installing a spar-type floating wind turbine can be divided into the following major stages:

(a) The catamaran approaches the pre-installed spar foundation;
(b) The crew wait for allowable weather;
(c) The catamaran gets connected to the spar foundation via sliding grippers;
(d) The lifting mechanism grips, lifts up, and transports a wind turbine assembly to the aft;
(e) The relative motion between the tower bottom and the spar top is

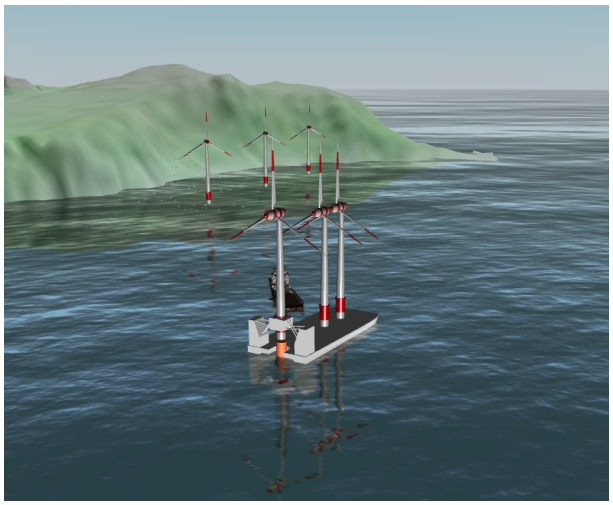

Fig. 1 Illustration of an offshore wind farm installed by the catamaran installation vessel.

monitored;
(f) The tower bottom and the spar foundation is mated;
(g) Bolting of the tower bottom takes place;
(h) The catamaran releases the spar foundation.

All critical stages should be evaluated to ensure technical feasibility of this installation concept. At stage (c), manual mode of the dynamic positioning (DP) system may be applied. After connection of the spar and the catamaran, the sliding grippers will only constrain the relative surge and sway motions of the two bodies but allow relative pitch and roll motions. Hatledal et al. (2017) focused on stage (c) and used the virtual prototyping framework Vicosim to study the contact forces between the grippers and the foundation. Jiang et al. (2018b) performed numerical analysis for stage (e) and identified factors affecting the relative motions in the horizontal plane. These studies are preliminary, and further numerical simulations and experiments are needed for assessment of the concept.
In this study, we focus on the mating phase (stage (f)) and investigate the relative heave motion between the lifted wind turbine assembly and the spar foundation. There are different methods to achieve heave compensation. Passive and active systems are two main categories, and hybrid active-passive systems also exist which combine features of both. Passive systems are mostly open-loop systems which do not require any energy input, and pneumatic-hydraulic systems are widely used (Huster et al., 2009). In contrast, active systems involve closed-loop control and require energy input. An active system usually involves electronics, sensors and controlled actuators, and should be used when the relative motion between two independently moving references need to be compensated (Woodacre et al., 2015). A great number of examples can be found regarding modeling and control of active hydraulic systems; see Korde (1998), Jelali and Kroll (2012) and Mintsa et al. (2012), and applications can be found in deep-water mining (Chung 2010) and lifting operation (Nam et al., 2013). Here, a representative hydraulic active heave compensator (AHC) is numerically modelled for the lifting mechanism of the whole system that consists of a dynamically positioned catamaran, a spar foundation with mooring lines, and sliding grippers.

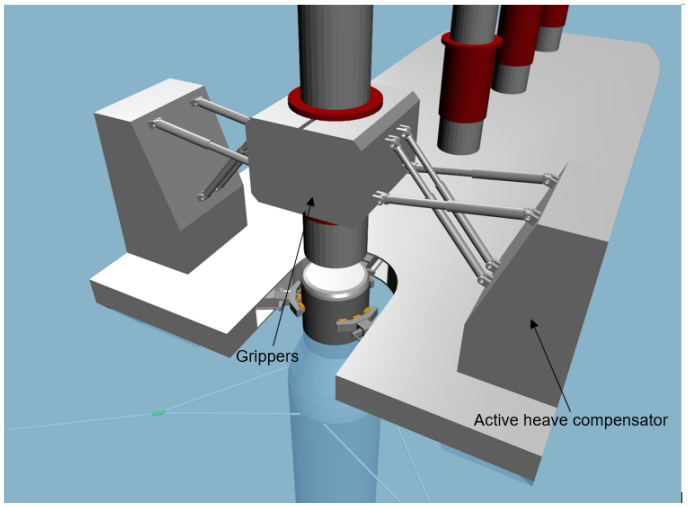

(a)

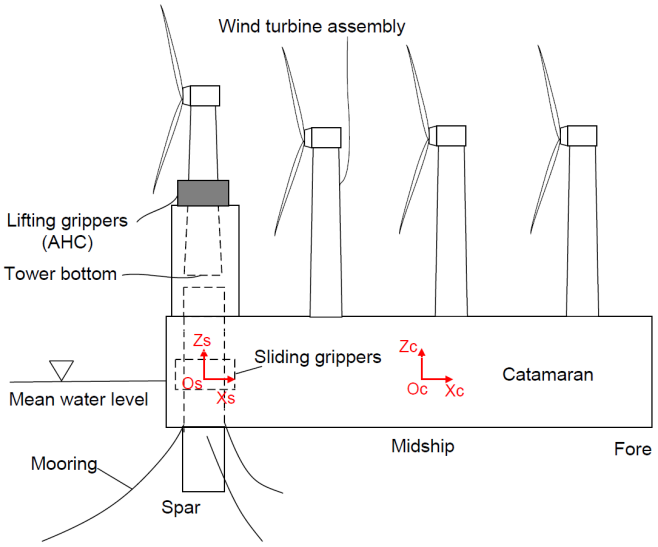

(b)

Fig. 2 Schematic of the mating of a wind turbine assembly (a) aft view (b) side view.

PROBLEM FORMULATION

Problem statement

As shown in Fig. 2, during the mating phase, the wind turbine assembly is gripped by the lifting grippers and laid upon the spar foundation. Because of the wave-induced motions on the catamaran and spar, uncontrolled landing of the wind turbine assembly on the spar foundation could result in large impact loads. To avoid this, motions of the lifting grippers should be controlled, compensating for the relative motions between the tower bottom and the spar top. The AHC should be located at both sides of the catamaran.
A hydraulic system is considered for the AHC consisting of a motor, a pump, valves, hydraulic fluid, and a hydraulic cylinder. Figure 3 gives an overview of the system components. In the figure, the wind turbine assembly is simplified as a mass, and the lifting grippers are represented by a cylinder connected to the wind turbine. Two right-hand coordinate systems are adopted, the global frame and the global vertical frame. The global coordinate system is fixed and initially aligned with body coordi-

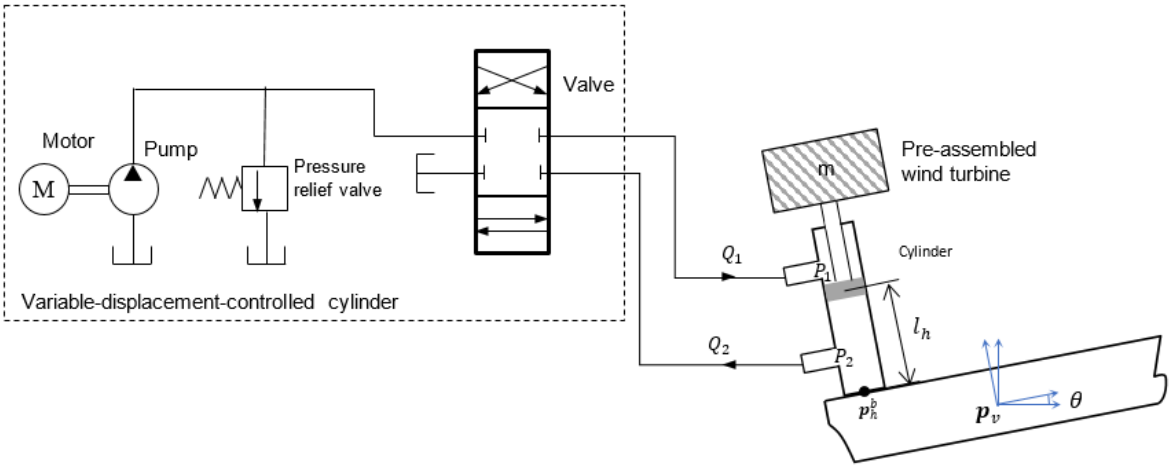

Fig. 3 Simplification of the AHC considered in the study.

nate system of the spar, with the origin point at the mean water level and x- and y-axes pointing to the north and east, respectively; see Fig. 2(b). In the body-fixed frame of the catamaran, the x^b- and y^b- axes point to the bow and port, respectively. It is assumed that the spar-top motions can be effectively measured by sensors, and the relative motions in pitch and roll are less important. The control objective is to reduce the relative heave motion between the tower bottom and the spar top in the global z-axis when exposed to oscillatory wave motions. The control input is the pump displacement.

System modelling

The main assumptions for the modelling are as follows:

- The reacting force from the hydraulic actuator does not influence the vessel motion;
- There is a rigid connection between the lifting grippers and the wind turbine assembly; see Fig.2(a);
- Hydraulic fluid density is constant;
- Pipeline distance is neglected;
- The effective bulk modulus of the hydraulic fluid is constant.

The position of the tower bottom in the global reference frame $\boldsymbol{p}_b$ becomes

$$\boldsymbol{p}_b = \boldsymbol{p}_v + \boldsymbol{R}(\boldsymbol{\Phi})(\boldsymbol{p}_h^b + \boldsymbol{d}_h), \tag{1}$$

where $\boldsymbol{p}_v$ stands for the position of the body origin of the catamaran in the global coordinate, $\boldsymbol{R}(\boldsymbol{\Phi})$ denotes the rotation matrix from the body-fixed to global reference frame parametrised by the Euler angle vector $\boldsymbol{\Phi}$, $\boldsymbol{p}_h^b$ is the position of the hydraulic lifting device in the body-fixed frame, and $\boldsymbol{d}_h = [0, 0, -l_h]^\top$ where $l_h > 0$ refers to the moving distance of the lifting grippers.
The velocity $\boldsymbol{v}_b$ of the tower bottom in the global frame is given by

$$\boldsymbol{v}_b = \boldsymbol{v}_v + \boldsymbol{R}(\boldsymbol{\Phi})\boldsymbol{S}(\boldsymbol{\omega}_v)(\boldsymbol{p}_h^b + \boldsymbol{d}_h) + \boldsymbol{R}(\boldsymbol{\Phi})\boldsymbol{v}_h, \tag{2}$$

where $\boldsymbol{v}_v$ is the velocity of the body origin of the catamaran in the global coordinate, $\boldsymbol{S}$ is a three-by-three skew-symmetric matrix used to represent cross products, and $\boldsymbol{v}_h = [0, 0, -\dot{l}_h]^\top$.
In this work, a simplified variable-displacement controlled cylinder is considered for the hydraulic system (Wang et al., 2012). As illustrated in Fig. 3, this cylinder will act as an equivalent of the actual system using a set of cylinders. The position of the cylinder is regulated by the oil pumped into and out of it. The load pressure P is defined as

$$P = \begin{cases} P_1 - P_r, & \text{if } P_1 > P_r \\ P_r - P_2, & \text{if } P_2 > P_r \end{cases} \tag{3}$$

where P_r denotes the return pressure which is considered to a constant, and P_1 and P_2 are the pressures on the two chambers of the cylinder.
The state-space equation of the one-degree variable displacement controlled cylinder system is

$$\dot{l}_h = v_h, \tag{4a}$$

$$\dot{v}_h = \frac{1}{m}(-f_c v_h + PA + F_{ext}), \tag{4b}$$

$$\frac{V}{\beta}\dot{P} = -Av_h - c_l P + u. \tag{4c}$$

where v_h denotes the moving velocity of the lifting grippers, m is the total mass including the mass of the hydraulic cylinder m_h and the mass of the turbine assembly m_t, f_c is the friction coefficient, A is the cross-section area of the cylinder, F_{ext} is the external force due to gravity of the turbine assembly, $V = V_0 + Al_h$ is the effective volume of the cylinder, V_0 is the fluid volume in the pipelines, β is bulk modulus of the hydraulic fluid, c_l is the fluid leakage coefficient, and u is equivalent to the axis rotating speed of the pump ω times pump displacement D_p.

FEEDBACK CONTROL SYSTEM

For the sake of simplification, the observer design is not included in this paper.

Trajectory generator

From Eq. (1), the desired length of the hydraulic piston l_{hd} is at the time instant t_k is calculated from

$$l_{hd}(t_k) = \left[\boldsymbol{p}_h^b - \boldsymbol{R}^\top(\boldsymbol{p}_s(t_k) - \boldsymbol{p}_v(t_k))\right]_3, \tag{5}$$

where $\boldsymbol{p}_s$ is the position of the spar top in the global reference frame, and $[\boldsymbol{a}]_3$ denotes the 3^{rd} element of the vector $\boldsymbol{a}$. A reference model is used to generate smooth trajectories $l_{hr}(t)$ and $\dot{l}_{hr}(t)$ for a series of desired lengths l_{hd}. The transfer function is given by

$$\frac{l_{hr}}{l_{hd}}(s) = \frac{\omega_r^3}{(s + \omega_r)(s^2 + 2\zeta_r\omega_r + \omega_r^2)}, \tag{6}$$

where s is the frequency, ζ_r denotes the damping ratio, and ω_r is a frequency parameter. $\zeta_r = 1$ is selected to ensure critical damping. The parameter ω_r influences the tacking speed, i.e., the higher the ω_r, the faster the tracking speed.
Because of the lowpass-filter characteristic of the reference system, there is a lag between the trajectory and the actual position. Its consequence is the unwanted impact during the final mating phase. To reduce this lag, a higher ω_r is needed. Otherwise, l_{hd} can be selected with a prediction over a short time horizon.

Control law design

In the control law design stage, it is assumed that the real-time measurements of the positions and orientations of the catamaran and spar are available. Because of the high bulk modulus β of the hydraulic fluid, $\frac{\beta}{V}$ has a large value that causes fast dynamics in the system. Therefore, the natural frequency for the system (4a)–(4b) is much smaller than for (4c). Singular perturbation theory is used to handle such problems in order to transfer the high-order system into a low-order model by dividing the system into a slow model and a fast model.
Define two error variables $e_1 = l_h - l_{hr}$ and $e_2 = \dot{e}_1 = v_h - \dot{l}_{hr}$. The system model with error dynamics is then given by

$$\left.\begin{aligned} \dot{e}_1 &= e_2 \\ \dot{e}_2 &= \tfrac{1}{m}(-f_c v_h + PA + F_{ext}) - \ddot{l}_{hr} \end{aligned}\right\} \quad \dot{\boldsymbol{e}} = f(\boldsymbol{e}, P), \tag{7a}$$

$$\varepsilon \dot{P} = -A(e_2 + \dot{l}_{hr}) - c_l P + u := g(\boldsymbol{e}, P, u), \tag{7b}$$

where Eq. (7a) is the slow model and Eq. (7b) is the fast model with $\boldsymbol{e} = [e_1, e_2]^\top$ and $\varepsilon = \frac{V}{\beta}$. As β gets very large, $\varepsilon \to 0$, and the isolated root of $g = 0$ is

$$\bar{P} = \frac{1}{c_l}(u - A\dot{l}_h) =: h_1(u) \tag{8}$$

Substituting $P = \bar{P}$ of Eq. (8) into Eq. (7a) yields,

$$\begin{aligned} \dot{e}_2 &= \frac{1}{m}[-f_c(e_2 + \dot{l}_{hr}) + \frac{A}{c_l}(u - A\dot{l}_h) + F_{ext}] - \ddot{l}_{hr} \\ &= \Upsilon u + \Psi, \end{aligned} \tag{9}$$

where $\Upsilon = \frac{A}{mc_l}$ and $\Psi = -\frac{A^2}{mc_l}\dot{l}_h + \frac{1}{m}(-d_h v_h + F_{ext}) - \ddot{l}_{hr}$. Υ is a positive constant by assuming that c_l is a constant.
Therefore the PID control law is given by

$$u = \frac{1}{\Upsilon}(-\Psi - c_1 e_1 - c_2 e_2 - c_3 \int e_1\, dt) := h_2(\boldsymbol{e}), \tag{10}$$

where c_1, c_2, and c_3 are positive constants. By using the pole placement technique, identical real eigenvalues are selected i.e., $\lambda_1 = \lambda_2 = \lambda^* < 0$. Hence, $c_1 = \lambda_1\lambda_2 = 2\lambda^*$ and $c_2 = -\lambda_1 - \lambda_2 = -2\lambda^*$. The integral control gain c_3 is tuned to handle the bias existed in the equilibrium points (8) caused by F_{ext} in u.

ANALYSIS PROCEDURE

Figure 5 shows the analysis procedure followed in this paper to assess the performance of the AHC on the mating process. Here, the coupled system refers to the catamaran, spar and positioning system. In the analysis, several sea states are selected for the numerical simulation first. Then, numerical simulations were performed in the time domain. Based on the simulation results, the absolute and relative heave motions between the spar top and the tower bottom will be analysed, and the effect of the AHC will be shown.

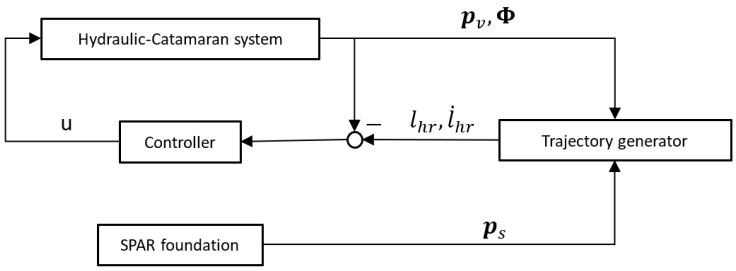

Fig. 4 Block diagram of the control system.

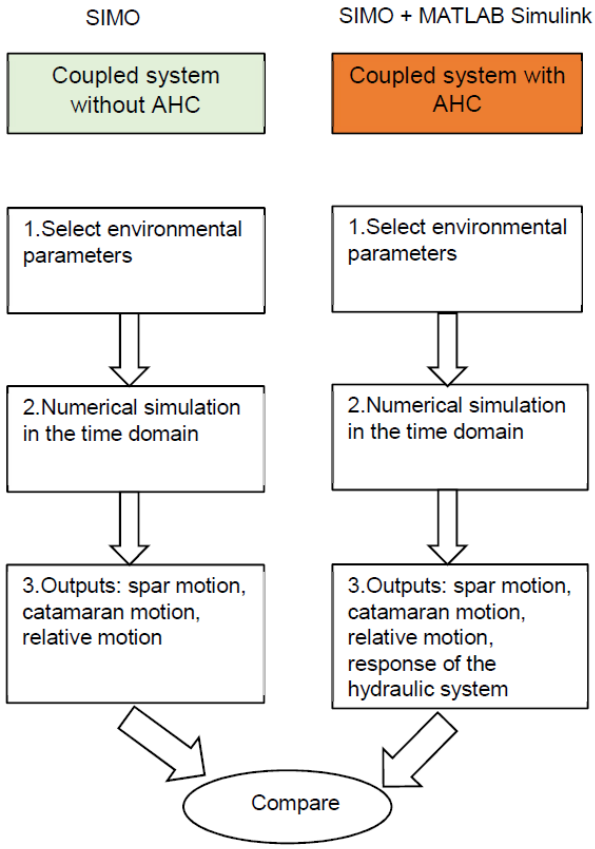

Fig. 5 Analysis procedure of the study.

NUMERICAL SIMULATION

The time-domain simulation program SIMO (MARINTEK, 2016) was used to simulate the coupled dynamic responses of the catamaran-spar system with 12 degrees-of-freedom. The catamaran installation vessel and the spar foundation were modelled as two rigid bodies connected by mechanical couplings (spring-damper system) at the vessel aft. The DP of the catamaran is realised by using four thrusters distributed along the vessel. A Kalman filter-based controller was used for the positioning system. In SIMO, the equations of motion of the two-body system are solved in the time domain, and the retardation functions are calculated using frequency-dependent added mass and damping. In this study, HydroD (Det Norske Veritas, 2011) was used to obtain these hydrodynamic coefficients. The second-order hydrodynamic loads in surge, sway, and yaw were calculated based on Newman's approximation. In addition, lin-

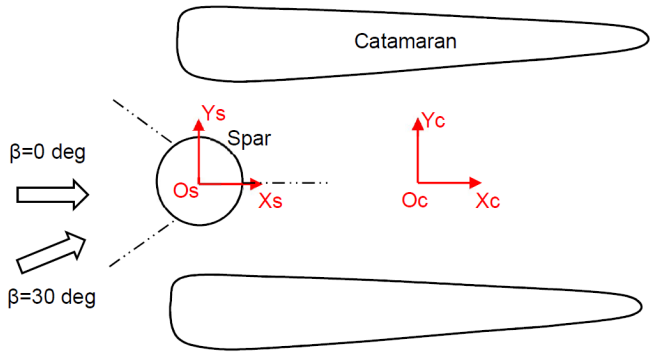

Fig. 6 Top view of the catamaran and spar at mean water level.

ear roll damping and quadratic yaw damping coefficients were specified for the catamaran to account for the viscous effects on the hull.
For the coupled system with lifting mechanism, MATLAB/Simulink was used to model the AHC, and motion responses of the catamaran and the spar from SIMO were used as inputs. In SIMO, the Newmark-Beta numerical integration method with a time step of 0.01 s was used. In MATLAB/Simulink, a 10^{-4} second sampling interval was adopted to accurately simulate the hydraulic system's fast dynamics. The control input update frequency is 10 Hz.

CASE STUDY

A catamaran vessel designed in the SFI MOVE project and a spar foundation based on the Hywind Scotland project (Steen, 2016) were considered in the case study. Figure 6 is a schematic of the initial positions of the bodies in the horizontal plane. In the figure, β denotes wave heading. The spar is constrained by a set of three mooring lines and connected to the catamaran via sliding grippers (not shown).
Tables 1–3 list the key parameters of the catamaran, wind turbine assemblies and spar. Prior to the mating operation, the spar top position, or the mating point, is located approximately 20 m above the waterline. A preliminary design of the hydraulic system was done, and the basic parameters of the hydraulic system are summarized in Table 4.

Table 1 Selected properties of the catamaran.

Parameter	*Symbol*	*Value*
Length overall (m)	L_{OA}	144
Breath moulded (m)	B	60
Draft (m)	T_c	8.0
Displacement mass (tonnes)	Δ_c	18502.9
Vertical centre of gravity (COG) above baseline (m)	KG_c	28.6
Body origin in global coordinate system (m)	(X_c,Y_c,Z_c)	(64,0,0)
Number of wind turbines on board	N_w	4

Table 5 lists the load cases under irregular waves. The significant wave height (H_S) of 2.0 m, and representative values of the spectral peak period (T_P) were chosen. A constant number of 3 was used in the directional function (Det Norske Veritas, 2010) for the directional short-crested wave spectrum, and the JONSWAP spectrum was used for wave generation. A water depth of 110 m was considered. For each load case,

Table 2 Selected properties of each wind turbine.

Parameter	*Symbol*	*Value*
Rated power (MW)	RP	10
Weight (tonnes)	M_w	1200
Hub height (m)	H_h	115

Table 3 Selected properties of the spar before mating.

Parameter	*Symbol*	*Value*
Diameter at top (m)	L_{bd1}	9.5
Diameter at waterline (m)	M_{bd1}	14
Draft (m)	T_{s1}	70
Vertical position of COG (m)	Zs_{COG1}	-51.8
Displacement mass (tonnes)	Δ_{s1}	11045
Vertical position of fairlead (m)	Z_{f1}	-15
Vertical position of mating point (m)	Z_m	20
Heave natural period (s)	T_{n3}	17.4

Table 4 Parameters of the hydraulic system.

Parameter	*Symbol*	*Value*
Cylinder cross-section area (m^2)	A	0.39
Bulk modulus (-)	β	$2e9$
Fluid leakage coefficient (-)	c_l	$1e$-7
Mass of the hydraulic piston (tonnes)	m_h	1
Friction coefficient (Ns/m)	f_c	$1e5$
Volume of fluid in the pipeline (m^3)	V_0	0.5

Table 5 Load cases (H_s=2.0 m).

LC	T_p	β	*AHC*
1	6.0	0	Yes, No
2	8.0	0	Yes, No
3	10.0	0	Yes, No
4	6.0	30	Yes, No
5	8.0	30	Yes, No
6	10.0	30	Yes, No

six 1800-s simulations with random seed numbers were performed, and the statistical results were obtained by averaging the six simulations.

RESULTS AND DISCUSSION

In this section, the simulation results of the load cases will be interpreted. The focus is to compare the relative heave motion of the mating point with and without AHC. Here, heave motion refers to the motion in the global z-direction, and heave velocity is time derivative of the heave motion.

Time series

Figures 7–8 show selected time series of the absolute heave motion and velocity of the tower bottom and the spar top. In the following, the tower bottom refers to the bottom position of the wind turbine assembly being held by the grippers. Without AHC, responses of the tower bottom were

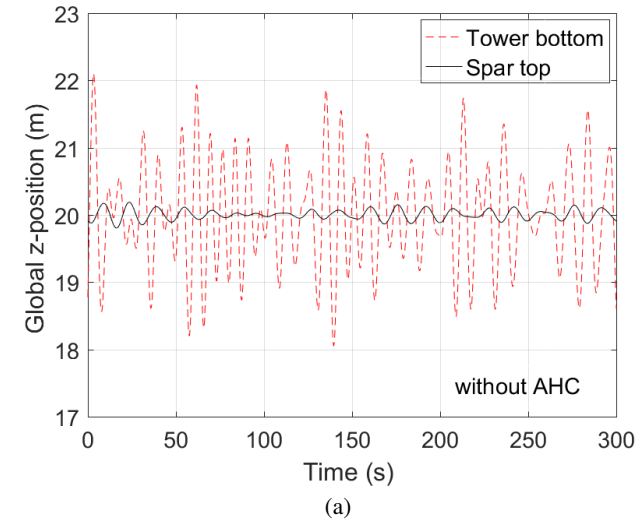

(a)

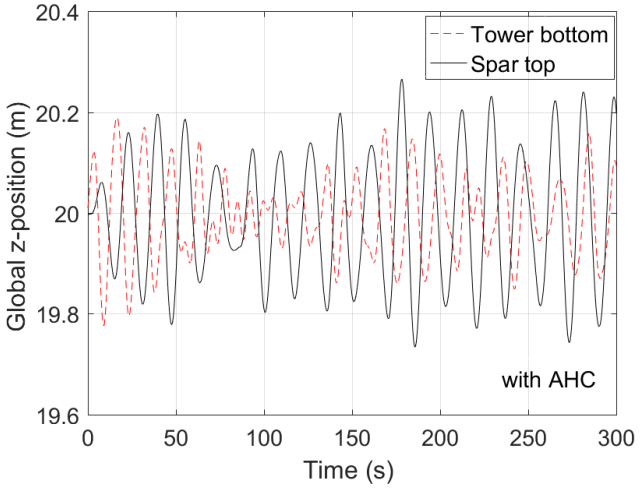

(b)

Fig. 7 Time history of the absolute heave displacement, H_S=2.0 m, T_P=10 s, β=0 deg, Seed 1 (a) without AHC (b) with AHC.

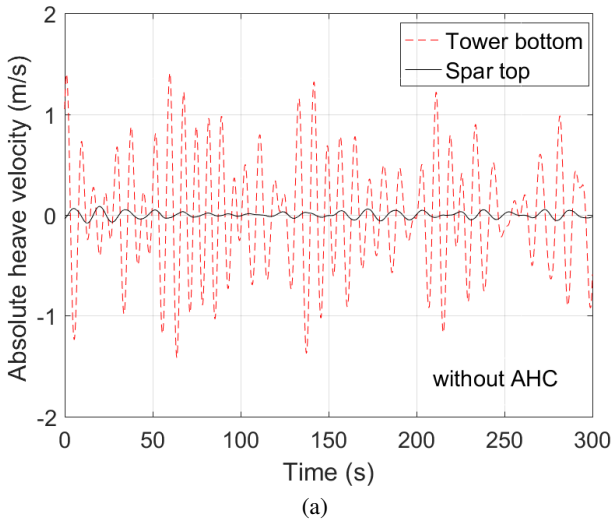

(a)

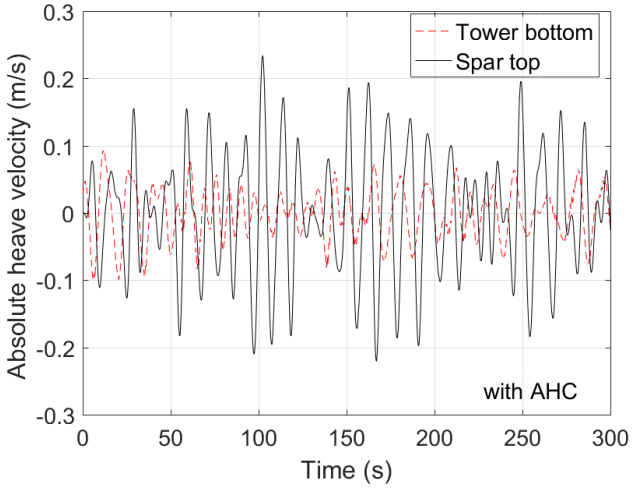

(b)

Fig. 8 Time history of the absolute heave velocity, H_S=2.0 m, T_P=10 s, β=0 deg, Seed 1 (a) without AHC (b) with AHC.

derived from rigid body motions of the catamaran, and the catamaran's heave and pitch motions contribute to the tower-bottom heave responses. As illustrated by the red dashed line in Fig. 7(a), this part is dominant compared to heave motion of the spar top. The spar-top motion is dominated by heave resonance of the spar. With AHC, heave motion of the tower bottom can be substantially compensated for, and there is generally good correspondence between the two curves in Figs. 7(b). Figure 8(a) compares the absolute heave velocities of the two bodies without AHC. Even for the short duration shown, the maximum heave velocity of tower bottom is well above 1 m/s. Because the aim of the AHC is to follow the spar-top heave motion which is quite small, AHC is also effective in reducing the heave velocity of the tower bottom (Fig. 8(b)). The maximum absolute heave velocity of the tower bottom is below 0.1 m/s in the time history.

The relative heave velocity is critical to the landing forces that occur during the mating. Figures 9–10 present the relative heave motion and velocity in the z-direction. Without AHC, the relative motion and velocity are comparable to the absolute ones. The magnitude of the relative velocity, in conjunction with the large weight of the wind turbine assembly (about 1200 tonnes) indicates great landing forces. With AHC, the relative velocity is on the order of 0.2 m/s, which is expected to be handled by the protection system during the mating process.

In Fig. 11(a), movements of the hydraulic piston are shown. The moving distance follows the wave-frequency heave responses of the tower bottom. In the case with H_S=2 m and T_P=10 s, the moving distance has a mean value of 3 m and maximum of 5.6 m. The moving distance is dependent on design of the hydraulic system and longitudinal location of the mating point along the catamaran. Fig. 11(b) plots the hydraulic load pressure at the cylinder side; this pressure varies around 30 MPa during the whole simulation.

As shown in Figures 12(a)–12(b), for the suspended wind turbine tower assembly, the gripper forces from the AHC are dominant, with the mean values close to the self weight. In comparison, the inertial forces are relatively small.

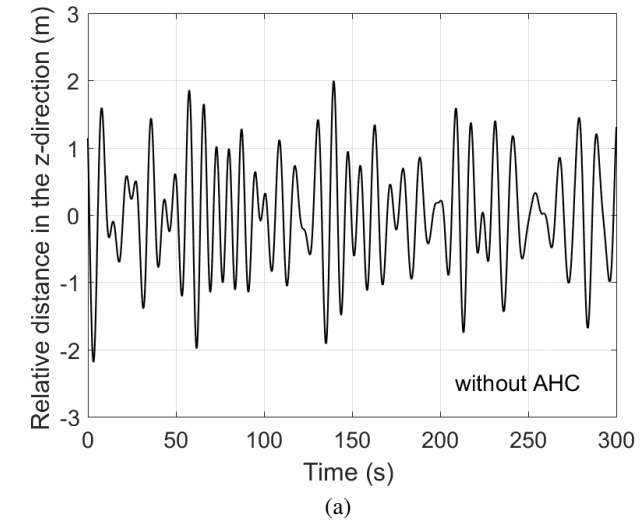

(a)

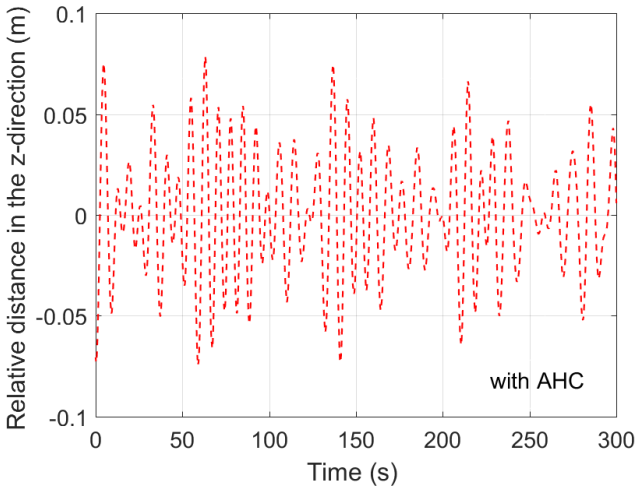

(b)

Fig. 9 Time history of the relative heave displacement between the spar top and the tower bottom, H_S=2.0 m, T_P=10 s, β=0 deg, Seed 1 (a) without AHC (b) with AHC.

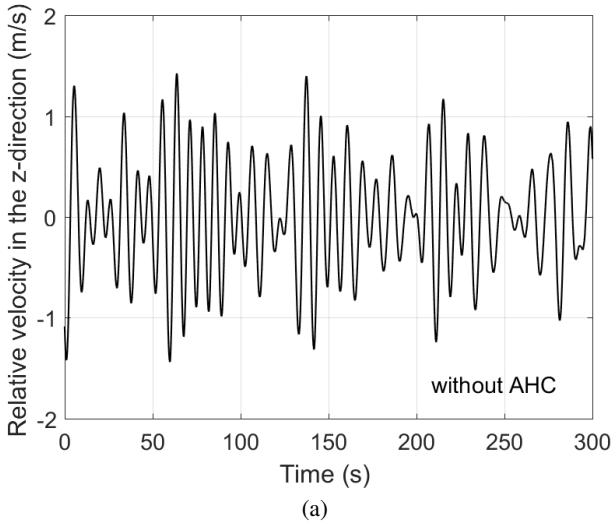

(a)

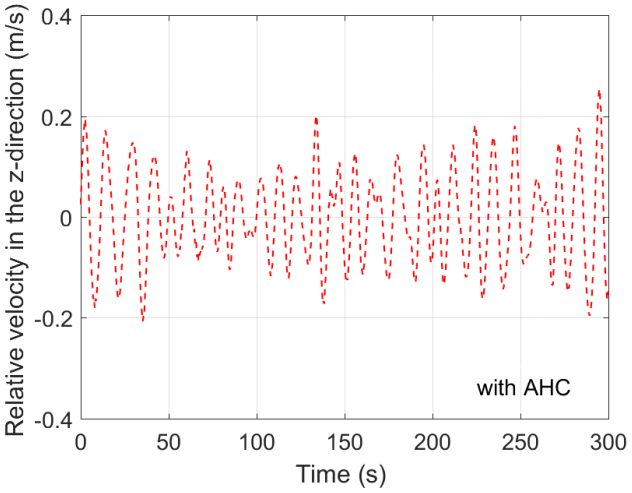

(b)

Fig. 10 Time history of the heave velocity of the tower bottom relative to the spar top, H_S=2.0 m, T_P=10 s, β=0 deg, Seed 1 (a) without AHC (b) with AHC.

Statistical results

Figures 13(a)–13(b) give the statistical average of the maximum responses during 1800 s. These maxima are simply the maximum values without extrapolations. The tower-bottom motions outweigh the spar-top motions for the system without AHC, and the maximum relative distance and relative velocity approaches the maximum tower-bottom displacement and velocity, respectively. Higher T_P is correlated with larger maximum relative response, primarily due to the shape of the JONSWAP spectrum and of the catamaran's pitch response amplitude operator (not shown). In practical marine operations, lower T_P is more often encountered.

Without the AHC, the maximum responses are sensitive to the wave heading, and β=0 deg gives greater responses. With the proposed AHC, the wave heading is expected to have less impact on the heave responses of the mating point. As shown in Figs. 14(a)–14(b), when β increases from 0 to 30 deg, the magnitude of this reduction is insignificant, although a reduction in the relative displacement or velocity is observed.

Landing forces

Like the landing of subsea structures on the seabed (Det Norske Veritas, 2014), the landing of the wind turbine assembly may cause structural damage to the spar deck or to the lifting mechanism, and the risks should be assessed. According to (Graczyk and Sandvik, 2012), the following approximation can be used to evaluate the maximum force in the lift wire for a component landing on the deck

$$F_{max} = m_t g + V_{rel}\sqrt{km_t}, \tag{11}$$

where F_{max} is the maximum force in the lift wire, g is the gravitational acceleration, V_{rel} is the relative velocity between the vessel and the load, and k is the equivalent stiffness of the deck and the lift wire. In the present case, stiffness of the lifting mechanism is not negligible.

Equation (11) implies the usefulness of AHC in reducing the landing forces during mating. When the maximum relative velocity of the wind turbine assembly is kept below 0.2 m/s, the second term could be rather small. On the other hand, a radial guiding system with soft stiffness may be pre-installed on the spar. Such a system can reduce the landing forces

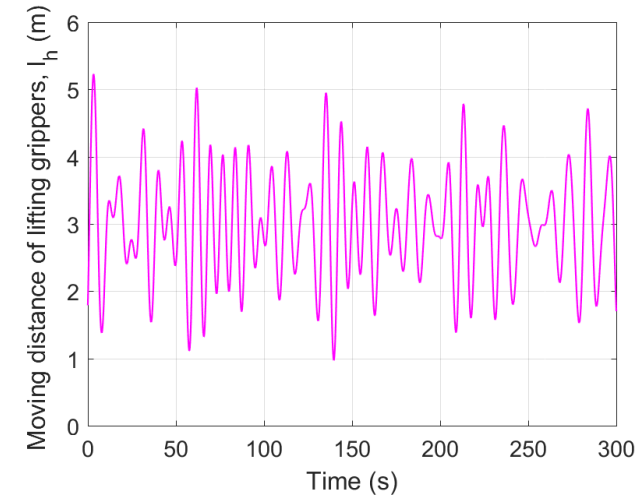

(a)

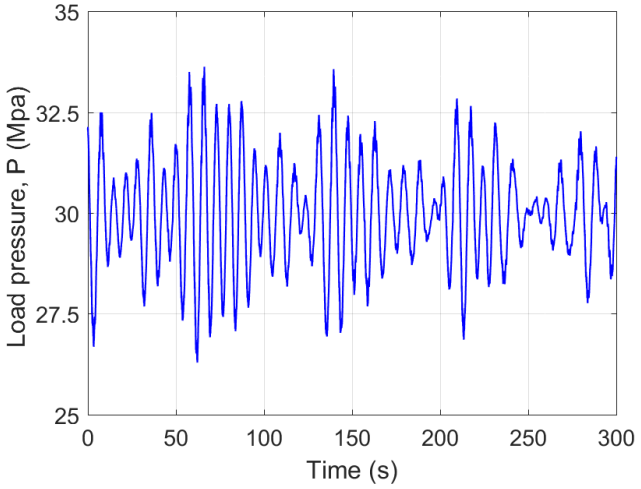

(b)

Fig. 11 Representative performance of the active heave compensator, H_S=2.0 m, T_P=10 s, β=0 deg, Seed 1 (a) moving distance of lifting grippers (b) hydraulic load pressure.

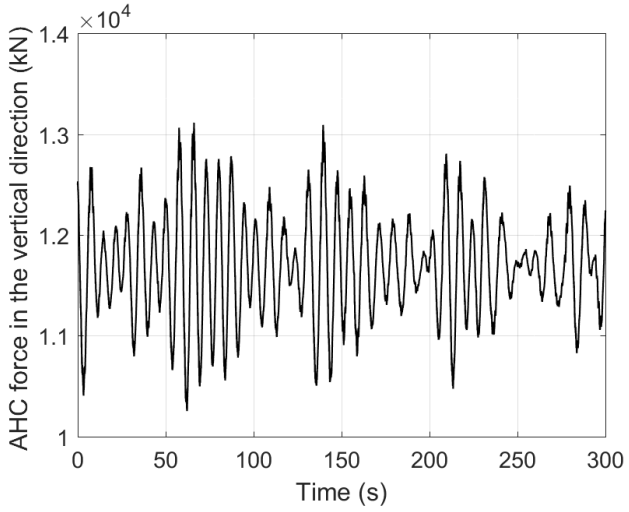

(a)

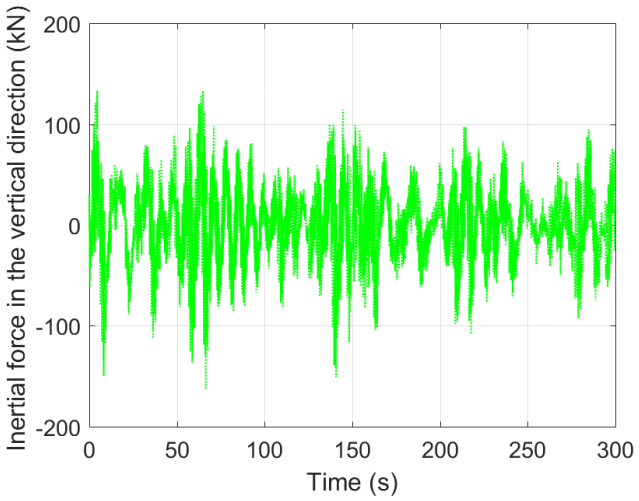

(b)

Fig. 12 Force components of the suspended tower assembly, H_S=2.0 m, T_P=10 s, β=0 deg, Seed 1 (a) gripper force (b) inertial force.

during the final contact. Because of the unknown contact stiffness, the landing forces are not calculated in this work.

CONCLUSION

This paper presents the modelling and simulation of an active heave compensator for a catamaran wind turbine installation vessel. The active heave compensator consists of a motor, a pump, valves, hydraulic fluid, and a hydraulic cylinder. Time-domain numerical simulations under irregular waves were conducted with an emphasis on the mating stage of the wind turbine installation process. A wind turbine assembly is being gripped by the lifting grippers and transferred onto a floating spar foundation.

The relative heave motion and velocity responses between the tower bottom and the spar top are compared for the cases with and without active heave compensator. It is shown that the active heave compensator can effectively reduce the relative heave velocity and can potentially improve the safety of the mating process.

ACKNOWLEDGEMENTS

This work was financially supported by the Research Council of Norway through the Centre for Research-based Innovation of Marine Operations(CRI MOVE, RCN-project 237929). The first author also thanks the Norwegian Ship-owners Association Fund at NTNU for the scientific travel grant.

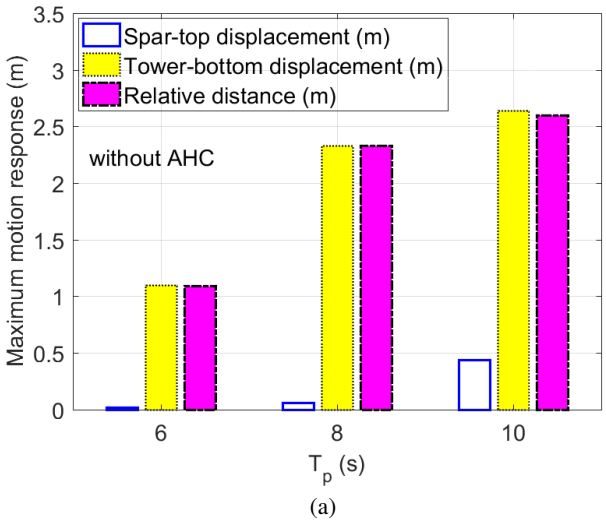

(a)

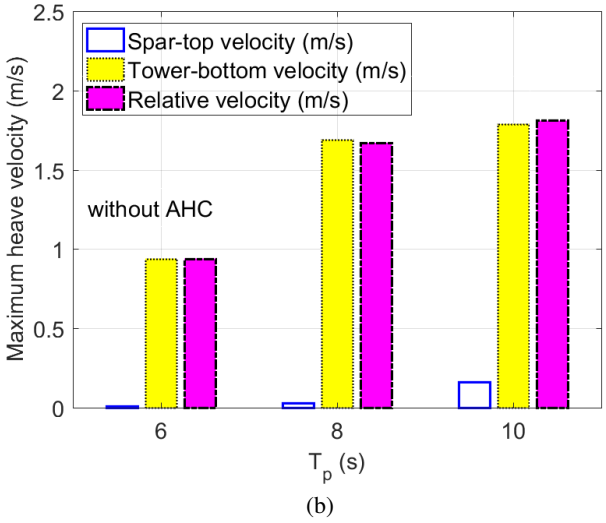

(b)

Fig. 13 Statistics of the simulation results without AHC, H_S=2.0 m, β=0 deg (a) maximum heave motion (b) maximum heave velocity.

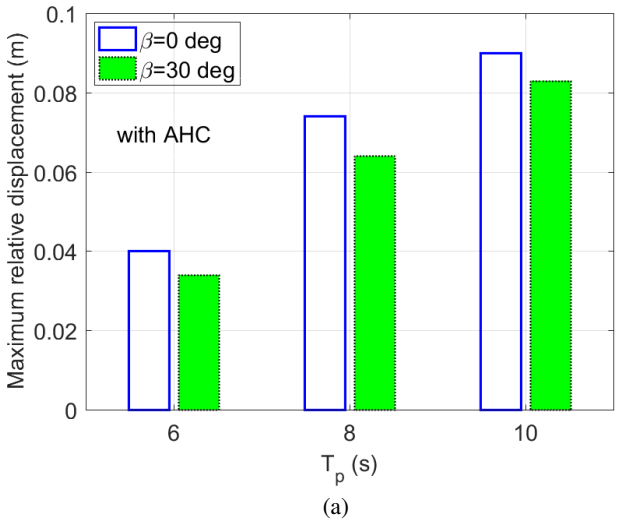

(a)

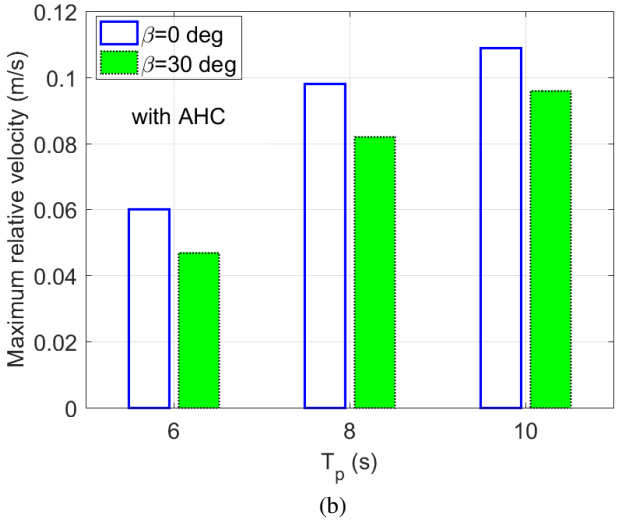

(b)

Fig. 14 Statistics of the simulation results with AHC, H_S=2.0 m (a) maximum relative heave displacement between the spar top and the tower bottom (b) maximum heave velocity between the spar top and the tower bottom.

REFERENCES

Acero, W G, Gao, Z, and Moan, T (2017). "Numerical study of a novel procedure for installing the tower and rotor assembly of offshore wind turbines based on the inverted pendulum principle ", *Journal of Marine Science and Application*, Vol 16, pp 243–260.

Chung, J S (2010). "Full-scale, coupled ship and pipe motions measured in north pacific ocean: The Hughes Glomar Explorer with a 5,000-m-long heavy-lift pipe deployed ", *International Journal of Offshore and Polar Engineering*, Vol 20, No. 1, pp 1–6.

Det Norske Veritas (2010). "Recommended Practice DNV-RP-C205 Environmental Conditions and Environmental Loads", Oslo, Norway.

Det Norske Veritas (2011). "SESAM user manual HydroD, program version 4.5".

Det Norske Veritas (2014). "Recommended Practice DNV-RP-H103 Modelling and Analysis of Marine Operations", Oslo, Norway.

Graczyk, M, and Sandvik, P C (2012). "Study of landing and lift-off operation for wind turbine components on a ship deck ", *ASME 2012 31ST International Conference on Ocean, Offshore and Arctic Engineering, OMAE2012-84273*, Rio de Janeiro, Brazil.

Hatledal, L I, Zhang, H, Halse K H, and Hilder, H P (2017). "Numerical simulation of novel gripper mechanism between catamaran and turbine foundation for offshore wind turbine installation ", *ASME 2017 36th International Conference on Ocean, Offshore and Arctic Engineering, OMAE2017-62342*, Trondheim, Norway.

Huster, A, Bergstrom, H, Gosior, J, and White, D (2009). "Design and operational performance of a standalone passive heave compensation system for a work class ROV ", *OCEANS 2009, MTS/IEEE Biloxi-Marine Technology for Our Future: Global and Local Challenges.*

Jiang, Z, Gao, Z, Ren, Z, Li, Y, and Duan, L (2018a). "A parametric study on the blade final installation process for monopile wind turbines under rough environmental conditions", *under review in Engineering Structures*.

Jiang, Z, Li, L, Gao, Z, Henning, K H, and Sandvik, P C (2018b). "Dynamic response analysis of a catamaran installation vessel during the positioning of a wind turbine assembly onto a spar foundation", *under review in Marine Structures*.

Jelali, M and Kroll, A (2012). "Hydraulic servo-systems: modelling, identification and control", *Springer Science & Business Media*.

Korde, U A (1998). “Active heave compensation on drill-ships in irregular waves ”, *Ocean Engineering*, Vol 25, Issue 7, pp 541–561.

MARINTEK (2016). “SIMO Version 4.8.4 - Theory Manual”.

Mintsa, H A, Venugopal, R, Kenne, J P, and Belleau, C (2012). “Feedback linearization-based position control of an electrohydraulic servo system with supply pressure uncertainty ”, *IEEE/ASME Transactions on Control Systems Technology*, Vol 20, Issue 4, pp 1092–1099.

Moné, C, Hand, M, Bolinger, M, Rand, J, Heimiller, D, and Ho, J (2017). “2015 Cost of wind energy review”, *Technical Report NREL/TP-6A20-66861*, National Renewable Energy Laboratory, CO, USA.

Nam, B W, Hong, S Y, Kim, Y S, and Kim, J W (2013). “Effects of passive and active heave compensators on deepwater lifting operation”, *International Journal of Offshore and Polar Engineering*, Vol 23, No. 1, pp 33–37.

Pineda, I, and Tardieu, P (2016). “The European offshore wind industry key trends and statistics 2016 ”, *https* : *//windeurope.org/about* − *wind/statistics/offshore/european* − *offshore* − *wind* − *industry* − *key* − *trends* − *and* − *statistics* − 2016/, Accessed: 2017-06-01.

Sarkar, A, and Gudmestad, O T (2013). “Study on a new method for installing a monopile and a fully integrated offshore wind turbine structure”, *Marine Structures*, Vol 33, pp 160–187.

Steen, K E (2016). “Hywind Scotland - status and plans”, *https* : *//www.sintef.no/projectweb/deepwind*$_2$016/*presentations*/, Accessed: 2017-02-01.

Wang, L, Book, W J, and Huggins, J D (2012). “Application of singular perturbation theory to hydraulic pump controlled systems ”, *IEEE/ASME Transactions on Mechatronics*, Vol 17, Issue 2, pp 251–259.

Woodacre, J K, Bauer, R J, and Irani, R A (2015). “A review of vertical motion heave compensation systems ”, *Ocean Engineering*, Vol 104, pp 140–154.